



HAL
open science

Atropisomerism in a 10-Membered Ring with Multiple Chirality Axes: (3 Z ,9 Z)-1,2,5,8-Dithiadiazecine-6,7(5 H ,8 H)-dione Series

Vesna Risso, Daniel Farran, Guilhem Javierre, Jean-Valère Naubron, Michel Giorgi, Patrick Piras, Marion Jean, Nicolas Vanthuyne, Roberta Fruttero, Dominique Lorcy, et al.

► To cite this version:

Vesna Risso, Daniel Farran, Guilhem Javierre, Jean-Valère Naubron, Michel Giorgi, et al.. Atropisomerism in a 10-Membered Ring with Multiple Chirality Axes: (3 Z ,9 Z)-1,2,5,8-Dithiadiazecine-6,7(5 H ,8 H)-dione Series. *Journal of Organic Chemistry*, 2018, 83 (15), pp.7566-7573. 10.1021/acs.joc.8b01009 . hal-01817538

HAL Id: hal-01817538

<https://hal.science/hal-01817538v1>

Submitted on 18 Jun 2018

HAL is a multi-disciplinary open access archive for the deposit and dissemination of scientific research documents, whether they are published or not. The documents may come from teaching and research institutions in France or abroad, or from public or private research centers.

L'archive ouverte pluridisciplinaire **HAL**, est destinée au dépôt et à la diffusion de documents scientifiques de niveau recherche, publiés ou non, émanant des établissements d'enseignement et de recherche français ou étrangers, des laboratoires publics ou privés.

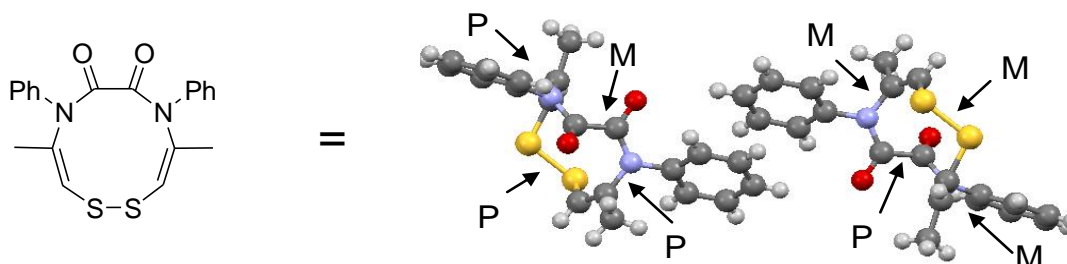
Atropisomerism in a ten-membered ring with multiple chirality axes: (3Z,9Z)-1,2,5,8-dithiadiazecine-6,7(5H,8H)-dione series

Vesna Risso,^a Daniel Farran,^{*a} Guilhem Javierre,^a Jean-Valère Naubron,^b Michel Giorgi,^b Patrick Piras,^a Marion Jean,^a Nicolas Vanthuynne,^a Roberta Fruttero,^c Dominique Lorcy,^d Christian Roussel^{*a}

- a) Aix-Marseille Univ, CNRS, Centrale Marseille, iSm2, Marseille, France.
b) Spectropole, Aix-Marseille Université, CNRS FR 1739, Marseille, France.
c) Department of Drug Sciences and Technology, University of Torino, Italy.
d) Univ Rennes, CNRS, ISCR – UMR 6226, F-35000 Rennes, France.

* Corresponding authors' e-mail address : christian.roussel@univ-amu.fr; daniel.farran@univ-amu.fr

Scheme of abstract:

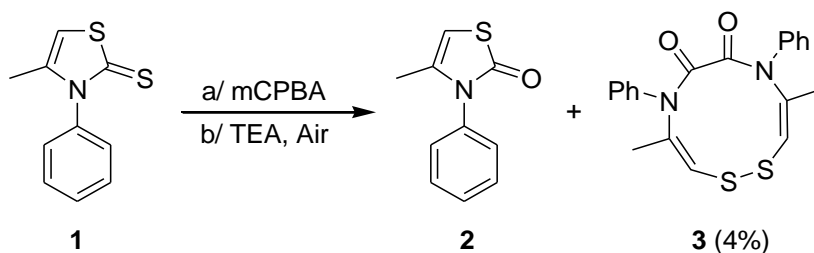


Abstract: For the first time, chirality in (3Z,9Z)-1,2,5,8-dithiadiazecine-6,7(5H,8H)-dione series was recognized. Enantiomers of the 4,9-dimethyl-5,8-diphenyl analogue were isolated at room temperature and their thermal stability determined. X-ray confirmed the occurrence of a pair of enantiomers in the crystal. Absolute configurations were assigned by comparing experimental and calculated vibrational/electronic circular dichroism spectra of isolated enantiomers. A distorted tesseract (four-dimensional hypercube) was used to visualize the calculated enantiomerization process which requires the rotation around four chirality axes. Conformers of higher energy as well as several concurrent pathways of similar energies were revealed.

Introduction

A classical method to prepare thiazoline-2-ones from the readily available corresponding thiazoline-2-thione goes through the formation of a thiazolium salt by alkylation at sulfur with an excess of alkylating agent. The crude thiazolium salt is then treated by sodium methylate in MeOH producing equimolecular amount of the thiazolinone and a methylthioether.¹ We were exploring a greener oxidation of the thiocarbonyl group in 4-methyl-3-phenyl-1,3-thiazole-2(3H)-thione **1** using *m*-CPBA or hydrogen peroxide so that the expelled sulfur atom will be in the form of water soluble sulfate (Scheme 1).² When *m*-CPBA is employed for the oxidation of thioether, the organic reaction medium

is usually neutralized with a NaHCO_3 aqueous solution.³ We treated first with aqueous NaOH solution to eliminate the formed *m*-CPBA salt and in the present case the expected sulfate. ^1H NMR of the crude in CDCl_3 showed the presence of unreacted thiazolinethione **1** and thiazolinone **2** thanks to the typical chemical shift of the coupled proton in position 5 at 6.33 and 5.85 ppm respectively. In addition, the analysis of the crude organic reaction medium was performed on a (*S,S*)-Whelk O1 chiral column which was installed in a ten chiral column screening unit equipped with on line CD and polarimeter detectors dedicated to routine enantiomer separation.⁴ (*S,S*)-Whelk O1 column is well known to separate enantiomers of atropisomeric thiazolinethiones and thiazolinones but also to discriminate thiazolinone from thiazolinethione on the basis of the different hydrogen bonding abilities of thiocarbonyl versus carbonyl groups in these heterocyclic systems.^{5,6} The UV trace showed a very clean crude reaction medium with two large peaks corresponding to the unreacted thiazolinethione **1** and the targeted thiazolinone **2** which were known in the laboratory.² In addition, two very minor extra peaks (*ca* 2% each) which were respectively eluted before and after the two main heterocycles attracted our attention (see SI). The CD (254 nm) detector trace was as expected silent for the two main compounds **1** and **2** but quite intriguingly two intense CD signals of opposite sign and similar intensity were associated to the two very minor peaks hardly detected in UV. These observations militated in favor of the formation of a very minor chiral by-product during the oxidation of achiral **1** into achiral **2**, a by-product (**3**) which enantiomers were nicely separated at room temperature and presented an intense CD response at 254 nm in the mobile phase. Column chromatography on silica and amylene stabilized CHCl_3 eluent allowed a clean isolation of **3** as the less retained compound. In this article, we disclose our full studies of the unusual stereochemical features of (*3Z,9Z*)-1,2,5,8-dithiadiazecine-6,7(*5H,8H*)-diones.⁷



Scheme 1. Oxidation of thiazoline-2-thione **1** yielding thiazolinone **2** and unknown **3** as a very minor compound

Results and Discussion

Chromatography of the isolated **3** on (*S,S*)-Whelk O1 column (Figure 1) confirmed that **3** was a racemate. The first eluted enantiomer was dextrorotatory according to a Jasco OR-4090 on line polarimeter, it also showed a positive CD sign at 300 nm. Several other commercially available chiral supports were additionally screened, the UV and CD traces as well as chromatographic parameters are given in the supporting information, the best separation was achieved on (*S,S*)-Whelk O1 column ($\alpha = 2.46$ and $R_s = 9.75$).

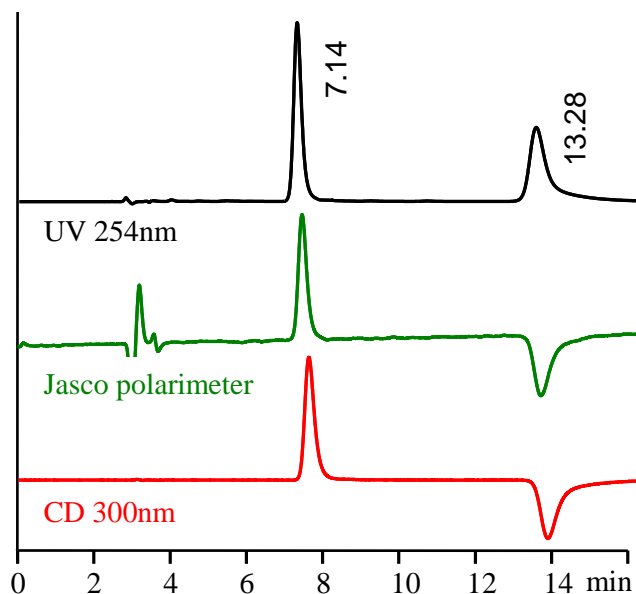
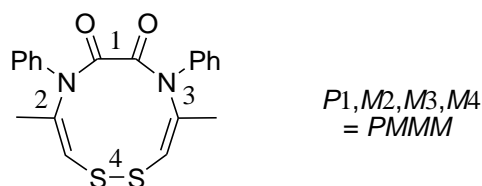


Figure 1. Chromatograms of racemic **3** on (*S,S*)-Whelk O1 column, 50:50 Heptane / EtOH, 25°C, 1 mL/min: $R_t(+)$ = 7.14, $R_t(-)$ = 13.28, $k(+)$ = 1.42, $k(-)$ = 3.50, $\alpha = 2.46$ and $R_s = 9.75$.

Single crystal X-ray analysis definitively identified **3** as (3*Z*,9*Z*)-4,9-dimethyl-5,8-diphenyl-1,2,5,8-dithiadiazecine-6,7(5*H*,8*H*)-dione (Scheme 2), in agreement with the HRMS data which proposed $C_{20}H_{18}N_2O_2S_2$ for element composition. The C_2 symmetry of the structure accounted for the deceptively simple 1H and ^{13}C NMR spectra: a single methyl peak (proton and carbon), a single $CH=$ (proton and carbon), a single carbonyl group and a single mono-substituted phenyl group (see SI).



Scheme 2. Definition of the four chirality axes. 1: oxamide axis, 2: left N-alkenyl axis, 3: right N-alkenyl axis, 4: disulfide axis. For instance the conformer having a *P* configuration for axis 1, *M* for axis 2, *M* for axis 3 and *M* for axis 4 (*P1,M2,M3,M4*) will be abbreviated in Figure 6 as *PMMM*.

The crystal structure (*C2/c*) showed four pairs of enantiomers in the cell for the same conformation (Figure 2).

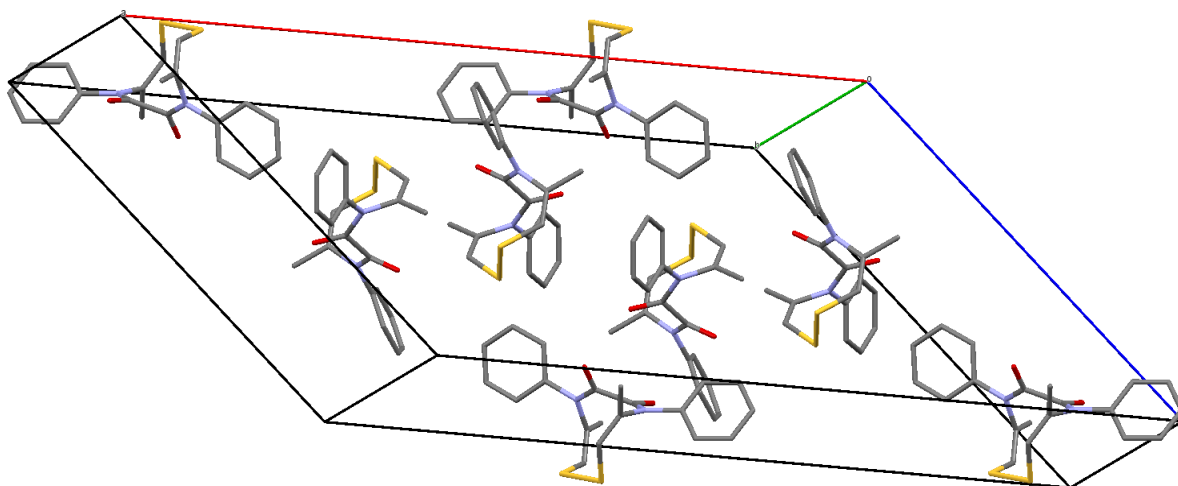


Figure 2. X-ray crystal structure of compound **3**. The cell contains four pairs of enantiomers (*C2/c*)

For sake of clarity, two enantiomers were selected among the eight available structures, they are displayed in Figure 3 with the *M* or *P* configuration labelling of each relevant axis. One can go from one enantiomer to the other by inverting the configuration around four axes: the oxamide bond, the disulfide bond and the two N-alkenyl ($C=C-N$) bonds. The amides are planar and thus the $C(O)-N$ axes apparently do not contribute to the local chirality descriptors of the ground state structure.

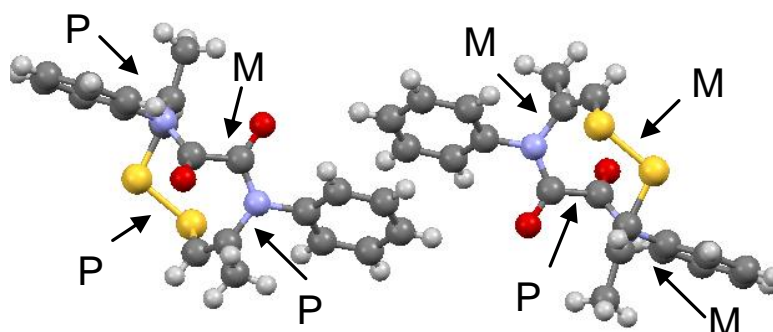


Figure 3. X-ray crystal structure of **3**: for sake of clarity only two enantiomers among the four pairs of enantiomers found in the cell are displayed. The *M* or *P* configuration of each axis is given.

Semi-preparative chiral chromatography on (*S,S*)-Whelk O1 column nicely afforded the two enantiomers of **3** (> 94% ee after careful evaporation of the collected fractions).

Inspection of the literature reveals that eleven derivatives having a (3*Z*,9*Z*)-1,2,5,8-dithiadiazecine-6,7(5*H*,8*H*)-dione framework have been characterized in ten articles since the seminal work of Baldwin and Walker in 1974 (Figure 4).⁸

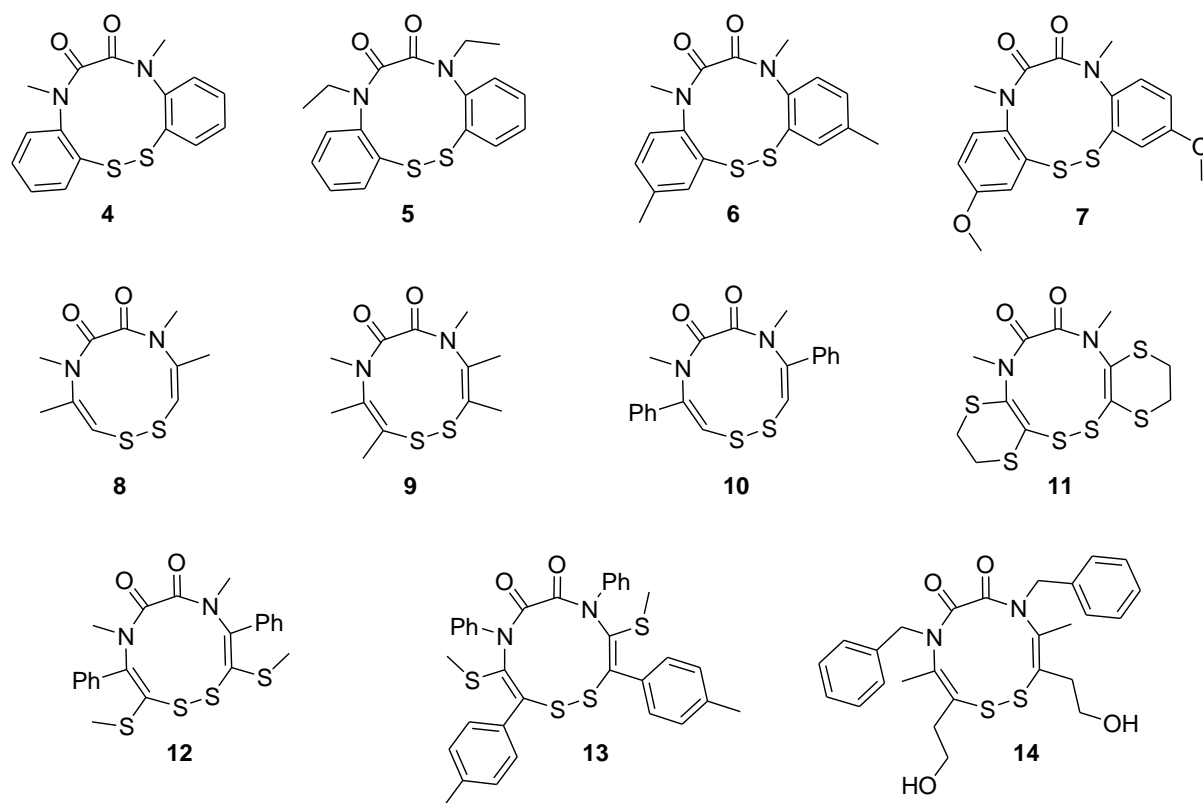


Figure 4. Display of the eleven (3*Z*,9*Z*)-1,2,5,8-dithiadiazecine-6,7(5*H*,8*H*)-dione derivatives reported in literature. **4**⁸⁻¹², **5**¹³, **6**^{9,11}, **7**^{9,11}, **8**^{9,11}, **9**^{9,11}, **10**^{9,11}, **11**¹⁴, **12**¹⁵, **13**¹⁶ and **14**.¹⁷

They mostly appeared in relation with the synthesis of diazadithiafulvalene derivatives resulting from the dimerization of the carbene ensuing from the basic treatment of 2-unsubstituted thiazolium or benzothiazolium salts. According to Itoh et coll. the bridging double bond in diazadithiafulvalene is then oxidized with molecular oxygen and the resulting addition peroxide rearranges to yield the corresponding (3*Z*,9*Z*)-1,2,5,8-dithiadiazecine-6,7(5*H*,8*H*)-dione derivative.¹¹ Itoh's mechanism was recently adapted to account for the formation of a (3*Z*,9*Z*)-1,2,5,8-dithiadiazecine-6,7(5*H*,8*H*)-dione derivative **14** from a vitamin B1 analogue.¹⁷ Thiazoline-2-thiones are known to produce 2-unsubstituted thiazolium salt under oxidation with H₂O₂ or *m*-CPBA,¹⁸ linking our experimental protocol (oxidation followed by TEA or NaOH treatment) to the previous formations of a ten membered ring.

It is quite remarkable that the chirality issues of the (3*Z*,9*Z*)-1,2,5,8-dithiadiazecine-6,7(5*H*,8*H*)-dione derivatives have been totally ignored in the handful of previous works. If truth be told, some clear evidences of the chirality in these series were already available from the reported single crystal X-ray structure determination or in some case from ¹H NMR spectra. Single crystal X-ray structure determination has been the preferred method to characterize the unfamiliar (3*Z*,9*Z*)-1,2,5,8-dithiadiazecine-6,7(5*H*,8*H*)-dione skeleton.^{8,9,11,13,14} Inspection of Cif files from the Cambridge database indicates that in all cases except one, two enantiomers could be clearly recognized in the cell while asymmetric conformations were mentioned for two compounds.¹⁰ The exception, which is even more appealing, is for compound **11** which crystallized in a P2₁2₁2₁ chiral group indicative of the probable occurrence of a conglomerate.¹⁴ ¹H NMR provided another obvious proof of the chirality of some of the literature samples which presented diastereotopic methylenic protons in ethyl or benzyl groups at room temperature. For instance, the ¹H NMR of compound **14** which was published in 2017 presented a nice AB spectra for the methylenic protons of the N-benzyl groups and a clear ABX2 motif for the methylene groups attached to the ethylenic bonds.¹⁷ These clear evidences of the chirality of the ten-membered ring conformer were completely unexploited. In these ten articles, there is definitively no mention of VT-NMR studies or chiral HPLC attempts in order to address the stability of the chiral conformers. The low barriers associated to oxamide inversion (see below) and disulfide inversion, one can find in the literature, might be at the origin of the lack of interest for chiral HPLC attempts to isolate stable enantiomers in **3** analogues.

Back to the first isolation of enantiomers in (3*Z*,9*Z*)-1,2,5,8-dithiadiazecine-6,7(5*H*,8*H*)-dione series, a key step was to establish the thermal stability of the enantiomers of **3** through the determination of the barrier to enantiomerization in dichloromethane. A barrier of 101.0 kJ/mol was obtained at 25°C, corresponding to a half-life time of 7.8 hours; such a barrier is high enough for a safe room temperature recording of chiroptical data of these unprecedented enantiomers. Table 1 shows the enantiomerization barriers and half-life times determined experimentally in four solvents at 30°C.

Solvent	$\Delta G^\ddagger_{\text{enantiomerization}}$ of 3 (kJ/mol, 30°C)	$t_{1/2}$ (at 30°C, in hours)
acetonitrile	99.2	1.9
ethanol	100.6	3.2
dichloromethane	101.0	3.8
chloroform	103.3	9.5

Table 1. Enantiomerization barriers and half-life times for **3** at 30°C in four solvents.

The barriers in chloroform were determined at 30°C and 61°C (See SI), they were not significantly different (103.3 and 103.5 kJ/mol respectively) pointing out a very small entropy contribution. Noteworthy, the barrier slightly but significantly decreases as solvent polarity increases: 103.3 kJ/mol in chloroform versus 99.2 kJ/mol in acetonitrile (Table 1).

Optical rotations were measured in chloroform: $[\alpha]_D^{25} = +1250 \pm 50$ (c 0.257, CHCl_3); $[\alpha]_{436}^{25} = +3300 \pm 100$ (c 0.257, CHCl_3) for (+)**3**, first eluted enantiomer on (*S,S*)-Whelk O1 and $[\alpha]_D^{25} = -1250 \pm 50$ (c 0.051, CHCl_3); $[\alpha]_{436}^{25} = -3300 \pm 100$ (c 0.051, CHCl_3) for (-)**3**, second eluted enantiomer. Molar rotations $[\Phi]_D^{25} = +$ or $-$ 4775 (c 0.257, CHCl_3) were in some aspects reminiscent of large rotations in helicene series.¹⁹

Circular dichroism spectra were recorded in order to determine the absolute configuration of (+)**3** and (-)**3** by comparing the calculated dichroism spectra for a chosen enantiomer with the experimental ones. Acetonitrile was the solvent for electronic circular dichroism (ECD) measurements while dichloromethane was used for vibrational circular dichroism (VCD). Calculations were performed for the optimized structure of the enantiomer having a (*M*) configuration around the oxamide bond, a (*P*) configuration around the disulfide bond and (*M*) configurations around both of the N-alkenyl bonds. The optimized structure for the single conformer was similar in terms of local configurations to the enantiomer originating from X-ray displayed on the right side of Figure 3. ECD calculations were performed using time dependent density functional theory (TD-DFT) with the SMD(CH_3CN)/CAM-B3LYP/6-31++G(d,p) // SMD(CH_3CN)/B3LYP/6-311G(d,p) level while VCD calculations were performed using density functional theory (DFT) with the SMD(CH_2Cl_2)/B3LYP/6-311+G(d,p) level (see supporting information for details). Experimental ECD spectra for (+)**3** and (-)**3** are reported in Figure 5. Nice mirror images were obtained. It is worth noting that the CD is positive for all the recorded wavelengths (185 to 350 nm) for (+)**3** and negative for (-)**3** in agreement with the same peak sign observed using polarimeter or CD detection during chromatography on chiral support. Calculated CD spectra for the (*M,P,P,P*) enantiomer is strictly negative for all the calculated range. A reasonable agreement is thus obtained between the calculated ECD spectra of the (*M,P,P,P*) enantiomer and the experimental ECD spectra of the second eluted enantiomer (-)**3**.

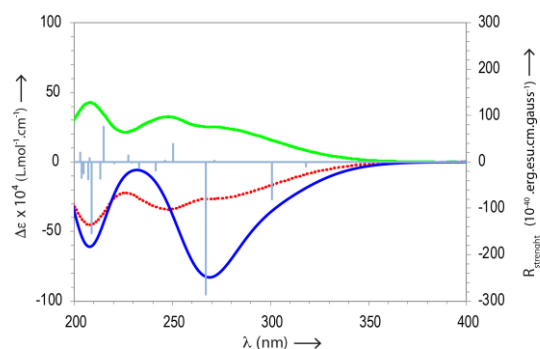


Figure 5. Experimental ECD spectra of (+)**3** (green curve, first eluted) and (-)**3** (red curve, second eluted) in acetonitrile (0.38 mmol/L) and calculated (blue curve) ECD for the optimized (*M,P,P,P*) enantiomer.

The experimental VCD spectra of (+)**3** and (-)**3** and calculated VCD spectra of the optimized (*M,P,P,P*) enantiomer are reported in Figure 6. The calculated VCD spectra is in good agreement with the experimental VCD spectra of (-)**3**.

In summary the two circular dichroism methods, ECD and VCD converged to safely assign the (*M,P,P,P*) absolute configuration to (-)**3**, the second eluted enantiomer on (*S,S*)-Whelk O1 column.²⁰

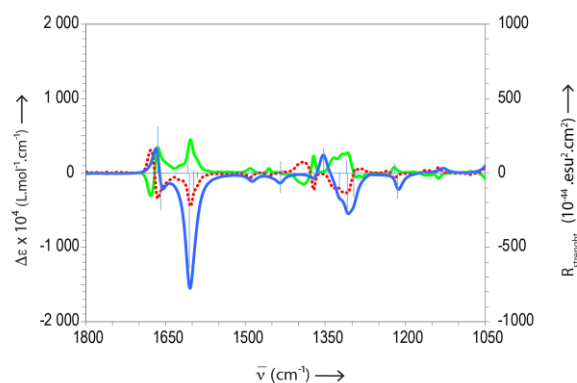


Figure 6. VCD spectra of (+)**3** (green curve, first eluted), (-)**3** (red curve, second eluted) and calculated VCD spectra of (*M,P,P,P*) enantiomer (blue curve).

DFT calculations (SMD(CH₂Cl₂)/B3LYP/6-311G(d,p)) were performed to visualize the inversion route of the four axes (*M,P,P,P*) into (*P,M,M,M*) paving the way of the enantiomerization process.²¹ Two main experimental features should be corroborated by calculations: the occurrence of a single pair of enantiomers and a barrier of 101.0 kJ/mol for the enantiomerization process in dichloromethane. Furthermore, the knowledge of the detailed process could be indicative of the required structural modifications which might, in future work, greatly affect the barrier and (or) promote the occurrence of other detectable conformational states. The nature (ground state (GS) or transition state (TS)) of each stationary point found along the reaction paths have been checked by a frequency calculation.

A distorted four-dimensional hypercube (distorted tesseract) which accounts for the inversion of 4 axes in a structure like **3** without a C₂ symmetry is given in Figure 7.²²

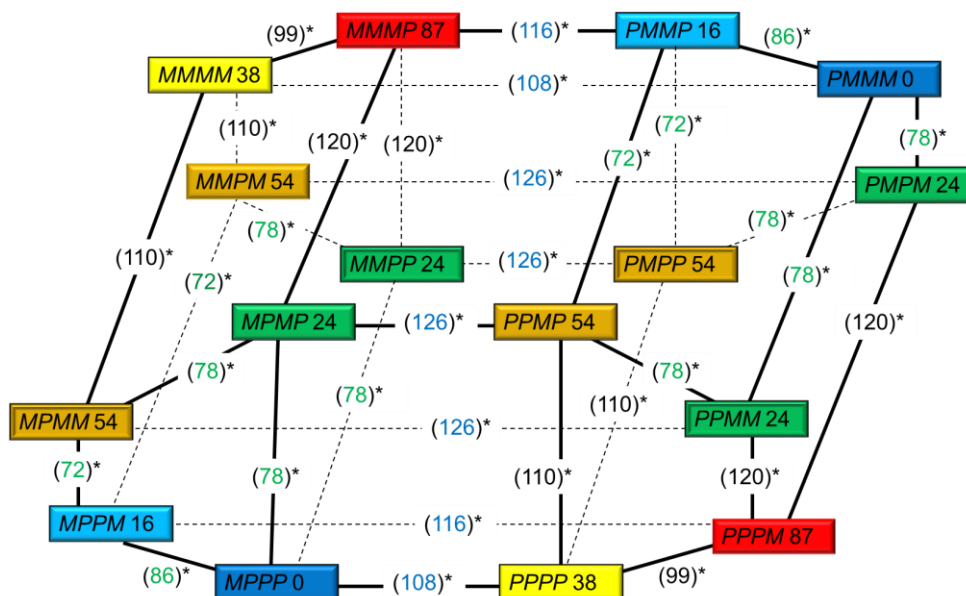


Figure 7. Display of the calculated conformer energies and barriers for compound **3** according to a distorted tesseract (distorted four-dimensional hypercube). Each stereoisomer is linked to four neighbors through inversion of configuration about a single axis. The values into brackets (*) correspond to the calculated Gibbs free energy at 298 K of the pass between two stereoisomers (kJ/mol), energetic references are *MPPP* and *PMMM* conformers as 0 kJ/mol. The configuration and the energy of the stereoisomers are given in the cartouches. All calculations were performed using SMD(CH₂Cl₂)/B3LYP/6-311G(d,p) theoretical level.

Each conformation is linked to four neighboring conformations differing by the chirality about a single axis. Eight pairs of enantiomers are thus defined and the inter-conversion of one enantiomer into its antipode requires at least four rotations. The front panel of the tesseract displays eight diastereoisomeric forms while the rear panel is composed of the corresponding enantiomers. The eight diastereoisomers associated to a (*M*) absolute configuration about the O=C-C=O axis are located on the West side of the figure and the eight enantiomers with a (*P*) configuration are located on the East side. The general scheme could have been simplified taking into account the C₂ symmetry in compound **3**: for instance *PMPM* and *PPMM* are identical and the two spots could have been merged in Figure 7; the same hold true for *PPMP* versus *PMPP*, *MPMM* versus *MMPM* and *MMPP* versus *MPMP*. That simplification is quite useful to save calculation power for both conformer energy and inter-conversion barrier but we prefer to display all the conformers to visualize all the inter-conversion pathways. Merging the identical conformers would lead to a superimposition of different routes and would hide the fact that there is no direct connection between twin conformers. The count of the different routes is important for the statistical correction of the calculated barrier when compared with the experimental one.

For sake of clarity, the calculated structures of individual conformers and transition states are displayed in the supporting information. All the displayed calculated energies in Figure 7 are given in kJ/mol at 298 K in CH₂Cl₂.

In Figure 7, the conformers are colored according to their energy: dark blue for the more stable and red for the less stable, the conformers with intermediate energies are colored in light blue, green, bright and dark yellow, respectively. Enantiomers display of course the same color, conformers which are superimposable due to the C₂ symmetry have the same color but they are differentiated by the relief of the cartouche. The *MPPP* and *PMMM* enantiomers in dark blue are the most stable (reference value 0 kJ/mol). They indeed correspond to the ones observed by X-ray and used for calculation of chiroptical properties. The light blue *MPPM* and *PMMP* enantiomers (16 kJ/mol) differ from the more stable by a single inversion along the disulfide bond. The energy gap is sufficient to explain that they were not detected during routine analyses and that a single conformer was included during VCD and ECD calculations. The calculated barrier is equal to 86 kJ/mol for the exchange major conformer (*MPPP*) to minor conformer (*MPPM*) via a direct inversion of the disulfide bond; as seen on the distorted tesseract, the exchange major conformer (*MPPP*) may be performed according to a less energetic three step route going through *MPMP* and *MPMM* conformers. These routes would have been difficult to trace without the display of the results on a distorted tesseract.

It is well documented that VT-NMR experiments can be used to detect two conformers in exchange when one of them is too low in concentration and thus escape detection. If the difference in chemical shifts is large enough and the barrier of exchange falls in the range of dynamic NMR, a broadening of the major signal occurs for a temperature range around coalescence.²³ Sixteen NMR spectra (500 MHz) of **3** were recorded in CDCl₃ between 235 and 315K and the height of the methyl peak was compared with that of the CHCl₃ peak taken as a reference. A very tiny deflection was indeed noticed around 295-285 K before a continuous change in relation with a T₂ broadening. Such a tiny deflection cannot be taken as a firm evidence of the exchange process but in the absence of exchange a strictly unbroken curve would have been obtained (See SI). These VT-NMR experiments militate in favor of the occurrence of very minor undetected conformer in exchange with a major conformer through a barrier (major-minor) producing a coalescence around 290K. These experiments fit quite well with the calculations.

The other conformers are of higher energy with a maximum value (87 kJ/mol) for the *MMMP* and *PPPM* pair.

The calculations also reveal a zone of relatively easy exchange between several diastereoisomeric forms having the same absolute configuration at the O=C-C=O axis with of course its counterpart in the enantiomeric space. These diastereoisomers are separated by calculated barriers ranging between 73 and 86 kJ/mol. These relatively low barriers are labeled in green in SW and NE parts of Figure 7.

The calculations show that depending on the starting conformer from the West part of the scheme, diastereoisomerization involving the rotation about the O=C-C=O axis calls for calculated barriers equal to 108, 116 or 126 kJ/mol to reach the East part of the scheme. If one excludes the four routes involving the oxamide axis inversion with a calculated barrier equal to 126 kJ/mol, two routes involving the inversion of the oxamide axis are calling for barriers equal to 116 kJ/mol and two

possibly preferred routes are calling for barriers equal to 108 kJ/mol. All these four routes bridging the West part to the East part of the scheme are all preceded or followed by N-alkenyl barriers of similar energy (110 kJ/mol). Thus the complete enantiomerization process between the observed *MPPP* and *PMMM* stable enantiomers proceeds through several quasi-isoenergetic routes in competition, most of them having a combination of inversion of the O=C-C=O axis and inversion of the N-alkenyl axes as a probable determining step. The slight but significant solvent effect on the barrier (Table 1) militates in favor of a sizeable contribution of the oxamide axis inversion as a determining step.

The literature is very poor in examples of cyclic oxamides forced to adopt a twisted *s-cis* conformation in the ground state and in which the inversion of the ring goes through a planar or close to planar *cis* conformation. To the best of our knowledge, the only example was reported by Isaksson and Liljefors who determined the barrier to enantiomerization in a series of seven membered cyclic oxamides **15** by dynamic NMR (Figure 8).²⁴ The barriers were in the range of 40 to 50 kJ/mol and thus *ca* 60 kJ/mol, lower than the one we determined in compound **3**.

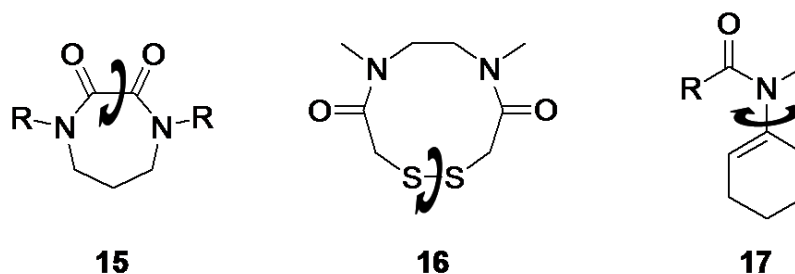


Figure 8. Selected model compounds from literature providing examples of barrier to inversion in oxamide **15**²⁴, disulfide linkage **16**²⁵ and N-alkenyl axis **17**.²⁶

Compound **16** provides a relevant example of disulfide linkage in a rather flexible ten membered ring.²⁵ Five conformers of similar energies were in equilibrium as seen in the NMR spectra. The barriers corresponding to the ring flip process, amide rotation and disulfide inversion were attained by dynamic NMR. The disulfide inversion had the lowest barrier: 72 kJ/mol. In compound **3**, the calculated disulfide inversions are in the 79-99 kJ/mol range depending on the backbone arrangement. As mentioned before, for some backbone arrangements, inversion around one of the N-alkenyl ((C=C)-N) axis produces calculated barriers in the same range as for the inversion of the O=C-C=O group providing additional determining steps in competition (Figure 6). Clark, Curran *et al.* recently reported a large series of barriers to rotation around the N-alkenyl bond in enamide framework **17** (Figure 8).²⁶ In the absence of large substituents in the vicinity of the N-alkenyl bond, the experimental barriers were in the 45-80 kJ/mol range.

In addition to compound **16**, other ten-membered rings presenting intracyclic amide group (heterocyclic analogues of dibenzodiazepines)²⁷ or exocyclic amide bond (ten-membered benzazecine derivative)²⁸ and additional insaturations showed enantiomeric conformations but the enantiomerization barriers obtained by VT-NMR were too low to imagine a room temperature isolation of the corresponding enantiomers.

The stepwise calculations reported in Figure 7 clearly show that the enantiomerization process in **3** may proceed through many routes of similar energy. The occurrence of several routes is quite rewarding when one compares the experimental value (101 kJ/mol in dichloromethane) with the calculated ones which are all higher in energy. It is worth recalling that the experimental energy of the barrier is lowered by $RT\ln(n)$ kJ/mol when n routes are in competition; the barrier calculations are thus in pretty good agreement with the experimental one. We are aware that some partially or totally concerted rotations around the different axes may also account for the observed barrier but the stepwise calculations reported in Figure 7 are a vivid source of inspiration for future work.

In conclusion we have isolated for the first time two enantiomers (atropisomers) in (3*Z*,9*Z*)-1,2,5,8-dithiadiazecine-6,7(5*H*,8*H*)-dione series and determined their thermal stability. The enantiomerization involves the inversion of configuration of four chirality axes. The chiroptical properties and absolute configuration have been determined. Calculations confirm that a single pair of enantiomers among the eight possible pairs is populated and that several routes are in competition for the enantiomerization process, most of them having the inversion about the O=C-C=O bond in combination with the N-alkenyl inversion for determining steps.

A completely unexplored field of investigation of these unusual chiral objects in which the chirality is arising from several linked chiral axes to form a ten membered ring is now open. The effect of chemical modifications of the reactive disulfide and oxamide groups on conformations and barriers to enantiomerization are underway and will be reported in due time.

Experimental Section

Synthesis of (3*Z*,9*Z*)-4,9-dimethyl-5,8-diphenyl-1,2,5,8-dithiadiazecine-6,7(5*H*,8*H*)-dione **3**:

a) oxidation with *m*-CPBA: to a solution of 4-methyl-3-phenyl-1,3-thiazole-2(3*H*)-thione **1** (400 mg, 1.9 mmol) in 3 mL CH₂Cl₂ (anhydrous), was added dropwise a solution of *m*-CPBA (1064 mg, 3.2 eq) in 30 mL CH₂Cl₂ (anhydrous) under stirring and nitrogen at 0°C. The reaction medium turned yellow and a solid was formed. 60 mL CH₂Cl₂ (anhydrous) were added to the flask for dissolution and the resulting mixture was treated with 40 mL (1M NaOH) solution at room temperature. The biphasic medium was stirred during 12 hrs at ambient. The recovered organic phase was washed three times with water (3 x 20 mL), dried on MgSO₄, filtered and evaporated. The resulting crude medium was analyzed by NMR and chiral chromatography (see text). Column chromatography on silica (eluent CHCl₃ amylene stabilized) afforded *ca* 15 mg of pure **3** as the first eluted compound.

b) oxidation with H₂O₂: to a solution of 4-methyl-3-phenyl-1,3-thiazole-2(3*H*)-thione **1** (518 mg, 2.50 mmol) in acetone (10 mL) was added H₂O₂ (30% in water, 1 mL, 2.50 mmol) and HPF₆ (1 mL) under nitrogen atmosphere and at 0°C. The reaction was then left in the same conditions for 30 min. The solvent was then partially removed by evaporation under reduced pressure and the crude was cooled at 0°C providing a solid which was collected by filtration (yellow solid) and immediately used in the next step without further characterization. To a solution of that solid in acetonitrile (50 mL) was

added dropwise a solution of triethylamine (0.70 mL, 5 mmol) in acetonitrile (25 mL) under nitrogen atmosphere. The reaction was then left under stirring overnight. The solvent was removed by evaporation under reduced pressure and dichloromethane (10 mL) was added. The organic layer was washed with water (20 mL), dried on MgSO₄ and evaporated under reduced pressure. The crude was purified by column chromatography (silica, eluent CHCl₃ -amylene stabilized-), yielding the desired product as a white solid (39 mg, 4% yield from 4-methyl-3-phenyl-1,3-thiazole-2(3*H*)-thione).

Note: compound **3** was first eluted with CHCl₃ (amylene stabilized) on silica. In all attempts, the chromatography was stopped after total elution of **3** and the composition of the remaining mixture was not further analyzed.

Mp = 212°C. Rf 0.38 (Silica plate, amylene stabilized CHCl₃). ¹H NMR (400 MHz, CDCl₃): δ 2.04 (s, 6H), 6.61 (s, 2H), 7.29-7.34 (m, overlapping 2H+4H), 7.41-7.47 (m, 4H). ¹³C NMR (100 MHz, CDCl₃): δ 21.8, 123.5, 126.0, 127.7, 129.5, 137.5, 152.7, 164.2. HMRS *m/z* calcd for [M+H]⁺ C₂₀H₁₉N₂O₂S₂⁺: 383.0882; found 383.0885.

Computational Details for the calculations of the IR/VCD and UV-vis/ECD spectra:

Spectra calculations have been performed using the single conformation of the *MPPP* enantiomer of **3**. The vibrational frequencies IR absorption and VCD intensities were calculated using the same theoretical level as for geometry optimisation SMD(CH₂Cl₂)/B3LYP/6-311+G(d,p). Computed harmonic frequencies have been calibrated using a scaling factor of 0.98 since they are generally larger than those experimentally observed. IR absorption and VCD averaged spectra were constructed from calculated dipole and rotational strengths assuming Lorentzian band shape with a half-width at half maximum of 10 cm⁻¹. Based on the SMD(CH₃CN)/B3LYP/6-311G(d,p) optimized geometries the ECD and UV spectra were calculated using time dependent density functional theory (TD-DFT) with CAM-B3LYP functional and 6-31++G(df,p) basis set. Calculations were performed for vertical 1A singlet excitation using 50 states. For a comparison between theoretical results and the experimental values the calculated UV and ECD spectra have been modeled with a Gaussian function using a half-width of 0.37 eV. Due to the approximations of the theoretical model used an offset almost constant was observed between measured and calculated frequencies. Using UV spectra all frequencies were calibrated by a factor of 0.97. All calculations were performed using Gaussian 16 package.²⁹

Computational Details for the calculations of the inversion mechanisms:

All the mechanisms have been calculated using DFT with B3LYP functional with 6-311G(d,p) basis set or cc-pvtz basis set, and PBE0 functional with 6-311G(d,p) basis set. The mean effects of the solvent (CH₂Cl₂) have been introduced using the SMD solvation model. The nature (ground state (GS) or transition state (TS)) of each stationary point found along the reaction paths have been checked by a frequency calculation. GS and TS have respectively none and a single imaginary frequency. Intrinsic reaction coordinate (IRC) calculations have been performed on each TS on both

direction in order to validate the reaction path. All calculations were performed using Gaussian 16 package.²⁹

Supporting information available: Copies of NMR spectra and chiral HPLC chromatograms. Kinetic of enantiomerization. X-Ray data. Optical rotations. ECD and VCD details. Computational details for the calculations of the IR/VCD and UV-vis/ECD spectra. Molecular modeling coordinates of conformers and transition states. Distorted tesseracts resulting from DFT calculations performed at the (SMD(CH₂Cl₂)/B3LYP/cc-pvtz and (SMD(CH₂Cl₂)/PBE0/6-311G(d,p) levels. Gibbs free energy, enthalpy and entropy values for every modeled GS and TS.

ACKNOWLEDGMENTS

VR thanks ERASMUS exchange program for support. CNRS and AMU fundings are acknowledged. The authors deeply thank Dr Valerie Monnier and Dr Gaetan Herbette from Spectropole Aix-Marseille Univ. for HMRS and NMR analytical support.

REFERENCES

- (1) (a) Roussel, C.; Adjimi, M.; Chemlal, A.; Djafri, A. Comparison of racemization processes in 1-arylpyrimidine-2-thione and 3-arylthiazoline-2-thione atropisomers and their oxygen analogs. *J. Org. Chem.* **1988**, *51*, 5076-5080. (b) Vanthuyne, N.; Andreoli, F.; Fernandez, S.; Roman, M.; Roussel, C. Synthesis, chiral separation, barrier to rotation and absolute configuration of *N*-(ortho-functionalized-aryl)-4-alkyl-thiazolin-2-one and thiazoline-2-thione atropisomers. *Lett. Org. Chem.* **2005**, *2*, 433-443.
- (2) Compounds **1** and **2** were available from a previous study: Roussel, C.; Suteu, C. Investigation into the chiral recognition mechanism of *N*-arylthiazolin-2(thi)one atropisomers on Chiralcel OJ by factorial design and lipophilicity approaches. *J. Chromatogr. A* **1997**, *761*, 129-138.
- (3) (a) Hussain, H.; Al-Harrasi, A.; Green, I.R.; Ahmed, I. Abbas, G.; Rehman N.U. meta-Chloroperbenzoic acid (mCPBA): a versatile reagent in organic synthesis. *RSC Adv.* **2014**, *4*, 12882-12917. (b) Karakuş, H.; Dürüst, Y. Novel benzothiophene 1,1-dioxide deoxygenation path for the microwave-assisted synthesis of substituted benzothiophene-fused pyrrole derivatives. *Mol. Divers.* **2017**, *21*, 53-60.
- (4) Vanthuyne, N.; Roussel, C. In *Differentiation of enantiomers part I* Ed. V. Schurig Book Series: *Topics in Current Chemistry* **2013**, *340*, 107-151.
- (5) (a) Pirkle, W.H.; Welch, C.J. Use of simultaneous face-to-face and face-to-edge π - π interactions to facilitate chiral recognition. *Tetrahedron Asymmetry* **1994**, *5*, 777-780. (b) Pirkle, W.H.; Koscho, M.E.; Wu, Z. High-performance liquid chromatographic separation of the enantiomers of *N*-aryloxazolinones, *N*-aryl thiazolinones and their sulfur derivatives on a synthetic chiral stationary phase. *J. Chromatogr. A* **1996**, *726*, 91-97 (c) Roussel, C.; Hart, N.; Bonnet, B.; Suteu, C.; Hirtopeanu, A.; Kravtsov, V.C.; Luboradzki, R.; Vanthuyne, N. Contribution of chiral HPLC in tandem with polarimetric detection in the determination of absolute configuration by chemical interconversion method: example in 1-(thi)oxothiazolinyl-3-(thi)oxothiazolinyltoluene atropisomer series. *Chirality* **2002**, *14*, 665-673.
- (6) (a) Abboud, J.L.M.; Roussel, C.; Gentric, E.; Sradi, K.; Lauransan, J.; Guiheneuf, G.; Kamlet, M.J.; Taft, R.W. Studies on amphiprotic compounds. 3. Hydrogen-bonding basicity of oxygen and sulfur compounds. *J. Org. Chem.* **1988**, *53*, 1545-1550. (b) Gentric, E.; Lauransan, J.; Roussel, C.; Metzger, J. Heteroassociation of heterocyclic amides and thioamides: selection by proton accepting and donating abilities. *New J. Chem.* **1980**, *4*, 743-746.
- (7) This work was presented in part as an oral communication during "Chirality 2015 ISCD-27 Boston" meeting, June 28-July 1, 2015, Boston USA.
- (8) Baldwin, J. E.; Walker, J. A. Competing [1-3]- and [3,3]-sigmatropic rearrangements of electron-rich olefins. *J. Amer. Chem. Soc.* **1974**, *96*, 596-597.
- (9) Itoh, T.; Nagata, K.; Okada, M.; Yamaguchi, K.; Ohsawa, A. The reaction of 3,3'-dimethyl-2,2'-bithiazolinium salts with superoxide. *Tetrahedron Lett.* **1992**, *33*, 6983-6986.
- (10) Yamaguchi, K.; Itoh, T.; Nagata, K.; Okada, M.; Ohsawa, A. Two novel ten-membered ring compounds: 1,2,5,8-dithiadiazecine-6,7-diones. *Acta Crystallographica, Section C: Crystal Structure Communications* **1993**, *C49*, 1514-1517.
- (11) Itoh, T.; Nagata, K.; Okada, M.; Ohsawa, A. Reaction of 3-methylthiazolium derivatives with superoxide. *Tetrahedron* **1993**, *49*, 4859-4870.
- (12) Lindamulage De Silva, A.; Risso, V.; Jean, M.; Giorgi, M.; Monnier, V.; Naubron, J-V.; Vanthuyne, N.; Farran, D.; Roussel, C. A Forgotten Chiral Spiro Compound Revisited: 3,3'-Dimethyl-3H,3'H-2,2'-spiro[[1,3]benzothiazole]. *Chirality* **2015**, *27*, 716-721.
- (13) Koizumi, T.; Bashir, N.; Kennedy, A. R.; Murphy, J. A. Diazadithiafulvalenes as electron donor reagents. *J. Chem. Soc., Perkin Transactions 1* **1999**, 3637-3643.

- (14) Eid, S.; Guerro, M.; Lorcy, D. 1,3-Thiazoline-2-thione-4,5-dithiolato, an efficient building block towards functionalized dithiadiazafulvenes. *Tetrahedron Lett.* **2006**, *47*, 8333-8336.
- (15) Morel, G.; Gachot, G.; Lorcy, D. Chemical and electrochemical investigations on the powerful π -electron donor dithiadiazafulvene: Isolation, spectroscopic characterization and charge-transfer complexation. *Synlett* **2005**, 1117-1120.
- (16) Bssaibis, M.; Robert, A.; Lemaguères, P.; Quahab, L.; Carlier, R.; Tallec, A. A new route to dithiadiazafulvene derivatives from mesoionic thiazoles. Formation of a ten-membered macrocycle by oxidation with oxygen and in situ generation of a charge transfer complex with tetracyanoquinodimethane. *J. Chem. Soc., Chem. Commun.* **1993**, 601-602.
- (17) (a) Liu, Y.; Wang, C.; Xue, D.; Xiao, M.; Liu, J.; Li, C.; Xiao, J. Reactions Catalysed by a Binuclear Copper Complex: Relay Aerobic Oxidation of N-Aryl Tetrahydroisoquinolines to Dihydroisoquinolones with a Vitamin B1 Analogue. *Chem. Eur. J.* **2017**, *23*, 3062-3066. (b) For a recent review on proton abstraction in thiamine analogues: Giovannini, P.P.; Bortolini, O.; Massi A. Thiamin-diphosphate-dependent enzymes as catalytic tools for the asymmetric benzoin-type reaction. *Eur. J. Org. Chem.* **2016**, 4441-4459.
- (18) Pesch, J.; Harms, K.; Bach, T. Preparation of axially chiral *N,N'*-diarylimidazolium and *N*-arylthiazolium salts and evaluation of their catalytic potential in the benzoin and in the intramolecular Stetter reactions. *Eur. J. Org. Chem.* **2004**, 2025-2035.
- (19) (a) Gingras, M.; Félix, G.; Peresutti, R. One hundred years of helicene chemistry. Part 2: stereoselective syntheses and chiral separations of carbohelicenes. *Chem. Soc. Rev.* **2013**, *42*, 1007-1050. (b) El Sayed Moussa, M.; Srebro, M.; Anger, E.; Vanthuyne, N.; Roussel, C.; Lescop C.; Autschbach, J.; Crassous, J. Chiroptical properties of carbo[6]helicene derivatives bearing extended π -conjugated cyano substituents. *Chirality* **2013**, *25*, 455-465. (c) Srebro, M.; Anger, E.; Moore II, B.; Vanthuyne, N.; Roussel, C.; Réau, R.; Autschbach, J.; Crassous, J. Ruthenium-Grafted Vinylhelicenes: Chiroptical Properties and Redox Switching. *Chem. Eur. J.* **2015**, *21*, 17100-17115. (d) Srebro-Hooper, M.; Jean, M.; Vanthuyne, N.; Toupet, L.; Williams, J.A.G.; Torres, A.R.; Riives, A.J.; Muller, G.; Autschbach, J.; Crassous, J. Synthesis and Chiroptical Properties of Hexa-, Octa-, and Deca-azaborahelicenes: Influence of Helicene Size and of the Number of Boron Atoms. *Chem. Eur. J.* **2017**, *23*, 407-418.
- (20) Polavarapu, P.L. Molecular Structure Determination Using Chiroptical Spectroscopy: Where We May Go Wrong? *Chirality*, **2012**, *24*, 909-920.
- (21) Additional DFT calculations were performed at the SMD(CH₂Cl₂)/B3LYP/cc-pvtz and SMD(CH₂Cl₂)/PBE0/6-311G(d,p) levels to comply with a reviewer demand. As expected for conformational analysis very minor changes in stereoisomer energies and interconversion barriers were observed, they do not significantly alter the general discussion based on the (SMD(CH₂Cl₂)/B3LYP/6-311G(d,p) level. The full resulting distorted tesseracts with conformer energies and barriers to interchange are given in the supporting information.
- (22) The tesseract presents 16 vertices and 32 edges, each edge being of the same length; in our work, it was largely distorted to place eight diastereoisomers in a front panel leading to the distorted tesseract displayed in Figure 7. For an example of the use of a four-dimensional hypercube (tesseract) in conformational analysis see: Alkorta, I.; Elguero, J. Conformational analysis of *N,N'*-dinaphthyl heterocyclic carbenes: imidazol-2-ylidenes and imidazol-2-ylidenes. *Struct. Chem.* **2011**, *22*, 1087-1094.
- (23) Sandström, J. "Dynamic NMR Spectroscopy" Academic Press 1982 pp 81-84.
- (24) Isaksson, R.; Liljefors, T. Conformations and barriers to inversion of seven-membered cyclic oxamides and their monothio and dithio analogs: a study by dynamic nuclear magnetic resonance spectroscopy and molecular mechanics. *J. Chem. Soc., Perkin Trans. 2* **1981**, 1344-1350.
- (25) (a) Maharajh, R.B.; Snyder, J.P.; Britten, J.F.; Bell, R.A. Synthesis, high-field NMR, x-ray structure, and conformational analysis of a 10-membered diamide disulfide ring. *Canadian J. Chem.* **1997**, *75*, 140-161. (b) Bain, A.D.; Bell, R.A.; Fletcher, D.A.; Hazendonk, P.; Maharajh, R.A.; Rigby, S.; Valliant, J. F. NMR studies of chemical exchange amongst five conformers of a ten-membered ring compound containing two amide bonds and a disulfide. *J. Chem. Soc., Perkin Trans. 2* **1999**, 1447-1453.
- (26) Clark, A.J.; Curran, D.P.; Fox, D.J.; Ghelfi, F.; Guy, C.S.; Hay, B.; James, N.; Phillips, J.M.; Roncaglia, F.; Sellars, P.B.; Wilson, P.; Zhang, H. Axially Chiral Enamides: Substituent Effects, Rotation Barriers, and Implications for their Cyclization Reactions. *J. Org. Chem.* **2016**, *81*, 5547-5565.
- (27) Costil, R.; Lefebvre, Q.; Clayden, J. Medium-sized-ring analogs of dibenzodiazepines by a conformationally induced Smiles ring expansion. *Angew. Chem. Int. Ed.* **2017**, *56*, 14602-14606.
- (28) Qadir, M.; Cobb, J.; Sheldrake, P.W.; Whittall, N.; White, A.J.P.; Hii, K.K.; Horton, P.N.; Hursthouse, M.B. Conformation Analyses, Dynamic Behavior, and Amide Bond Distortions of Medium-sized Heterocycles. 2. Partially and Fully Reduced 1-Benzazocines, Benzazonines, and Benzazecines. *J. Org. Chem.* **2005**, *70*, 1552-1557.
- (29) Gaussian 16 Revision A.03: Frisch, M.J.; Trucks, G.W.; Schlegel, H.B.; Scuseria, G.E.; Robb, M.A.; Cheeseman, J.R.; Scalmani, G.; Barone, V.; Petersson, G.A.; Nakatsuji, H.; Li, X.; Caricato, M.; Marenich, A.V.; Bloino, J.; Janesko, B.G.; Gomperts, R.; Mennucci, B.; Hratchian, H.P.; Ortiz, J.V.; Izmaylov, A.F.; Sonnenberg, J.L.; Williams-Young, D.; Ding, F.; Lipparini, F.; Egidi, F.; Goings, J.; Peng, B.; Petrone, A.; Henderson, T.; Ranasinghe, D.; Zakrzewski, V.G.; Gao, J.; Rega, N.; Zheng, G.; Liang, W.; Hada, M.; Ehara, M.; Toyota, K.; Fukuda, R.; Hasegawa, J.; Ishida, M.; Nakajima, T.; Honda, Y.; Kitao, O.; Nakai, H.; Vreven, T.; Throssell, K.; Montgomery, J.A.; Peralta, Jr.J.E.; Ogliaro, F.; Bearpark, M. J.; Heyd, J.J.; Brothers E.N.; Kudin, K.N.; Staroverov, V.N.; Keith, T.A.; Kobayashi, R.; Normand, J.; Raghavachari, K.; Rendell, A.P.; Burant, J.C.; Iyengar, S.S.; Tomasi, J.; Cossi, M.; Millam, J.M.; Klene, M.; Adamo, C.; Cammi, R.; Ochterski, J.W.; Martin, R.L.; Morokuma, K.; Farkas, O.; Foresman, J. B.; Fox, D.J. Gaussian Inc. Wallingford CT 2016.